



Optical cryomicroscopy and differential scanning calorimetry of buffer solutions containing cryoprotectants

Astrid Hauptmann^{a,b}, Georg Hoelzl^a, Thomas Loerting^{b,*}

^a Sandoz GmbH, Biochemiestr. 10, 6336 Langkampfen, Austria

^b Institute of Physical Chemistry, University of Innsbruck, Innrain 52c, 6020 Innsbruck, Austria

ARTICLE INFO

Keywords:

Cryoprotectants
Drug formulation
Glass transition temperature
Cryomicroscopy
Differential scanning calorimetry
Ice crystallization
Freezing
Thawing
Buffer solution
Freeze damage

ABSTRACT

In the pharmaceutical industry, cryoprotectants are added to buffer formulations to protect the active pharmaceutical ingredient from freeze- and thaw damage. We investigated the freezing and thawing of aqueous sodium citrate buffer with various cryoprotectants, specifically amino acids (cysteine, histidine, arginine, proline and lysine), disaccharides (trehalose and sucrose), polyhydric alcohols (glycerol and mannitol) and surfactants (polysorbate 20 and polysorbate 80). Hereby, we employed optical cryomicroscopy in combination with differential scanning calorimetry in the temperature range to -80 °C. The effect of cryoprotectants on the morphology of the ice crystals, the glass transition temperature and the initial melting temperature is presented. Some of the cryoprotectants have a significant impact on ice crystal size. Disaccharides restrict ice crystal growth, whereas surfactants and glycerol allow ice crystals to increase in size. Cysteine and mannitol cause dehydration after thawing. Either one or two glass transition temperatures were detected, where arginine, surfactants, glycerol, proline and lysine suppress the second, implying a uniform freeze-concentrated solution. The initial melting temperature of pure buffer solution can be shifted up by adding mannitol, both disaccharides and both surfactants; but down by glycerol, proline and lysine.

1. Introduction

In the 1940s–1970s cryoprotectants such as polyhydric alcohols (e. g., glycerol, mannitol), and sugars (e. g., sucrose, maltose, mannose, fructose, glucose, etc.) were added to aqueous solutions in order to stabilize macromolecules during freezing [1–4]. Certain protectants prevent an enzyme to lose its efficacy [2], avoid irreversible aggregation [4] or stabilize the native structure [5]. Since then, cryoprotectants have brought major benefits in all kinds of fields. To mention some examples, in food technology, they ensure quality and shelf life of frozen foods by suppressing ice crystal growth and preventing disruption of tissue [6–8]. In the automotive industry, they serve as an antifreeze additive in water-based liquids [9]. In cryobiology, they improve viability and functionality of bacteria cultures [10,11] and cell lines [12,13]. In nature, cryoprotectants are often antifreeze proteins produced by animals, plants or other organisms, which prevent growth and recrystallization of ice by binding to small ice crystals [14–16]. Even though nature is showing us many examples, most of the cryoprotectants employed in pharmaceutical industry are carbohydrates [17,18].

Here we investigate substances that can potentially be used as

cryoprotectants in protein therapeutics. There are three different hypotheses about the cryoprotective effect on proteins:

1. The “*water substitute hypothesis*”: The thermodynamic stability of the protein is ensured through hydrogen bonds. Cryoprotectants containing free hydroxyl groups allow maintaining these hydrogen bonds even after removal of water so that also the dried protein remains in its native state [19–21]. This hypothesis explains the cryoprotective effect of excipients during freeze-drying.
2. The “*glassy state hypothesis*”: In the vitrified, glassy state degradation processes take place at an insignificant rate. The liquid-to-glass transition temperature of the freeze-concentrated solution (T_g' of FCS) is, therefore, of key importance. Hereby, sugars serve as anti-plasticizer so that the glassy state is achieved at higher temperatures, and the protein is immobilized in a rigid sugar matrix [22,23].
3. The “*preferential exclusion hypothesis*”: Carbohydrates are preferably excluded from the surface of the protein. Consequently, the protein is surrounded by an almost carbohydrate-free shell and becomes more hydrated. As a result, the protein is protected against denaturation [24–26].

* Corresponding author.

E-mail addresses: astrid.hauptmann@novartis.com (A. Hauptmann), georg.hoelzl@novartis.com (G. Hoelzl), thomas.loerting@uibk.ac.at (T. Loerting).

<https://doi.org/10.1016/j.ejpb.2021.03.015>

Received 27 November 2020; Received in revised form 21 March 2021; Accepted 27 March 2021

Available online 2 April 2021

0939-6411/© 2021 The Author(s). Published by Elsevier B.V. This is an open access article under the CC BY license (<http://creativecommons.org/licenses/by/4.0/>).

In the present study the focus is on the glassy state hypothesis. By using buffer solutions containing no protein, we do not have any effects arising from preferential exclusion from the protein. Also, we study solutions without drying, so that water substitution does not play any role. The focus here is on how the cryoprotectant shifts the glass transition temperature(s) of the freeze-concentrated solutions and how the ice crystal morphology is affected through cryoprotectants. Some additives investigated, like sorbitol and mannitol, may not be appropriate cryoprotectants in protein solutions since they are prone to crystallize themselves during cooling. This may then lead to a disadvantageous phase separation jeopardizing protein protection [27–29]. By contrast, disaccharides in formulations have proven to be effective [30,31] with the exception of trehalose, where crystallization of trehalose dihydrate may occur [32,33]. Glycerol and sucrose have a stabilizing effect on the protein by lowering the freezing temperature and decreasing the affinity of protein to adsorb at container walls or ice crystals. Hence, adsorption-induced structural unfolding of protein can be opposed [34].

All of the previous studies on cryoprotectants must be treated with due caution since the freeze and thaw behavior always depends on more than just one factor. Initial pH, cooling/heating rates and concentration of excipients must be determined on a case to case basis. For our study we have chosen to investigate five amino acids (cysteine, histidine, arginine, proline and lysine), two disaccharides (trehalose and sucrose), two polyhydric alcohols (glycerol and mannitol) and two surfactants (polysorbate 20 and polysorbate 80). Table 1 lists these cryoprotectants together with their mechanisms of cryoprotection reported in literature [17,35–76].

When aqueous solutions cool to subzero, two main events take place in many cases: Firstly, the crystallization of water to ice at the freezing temperature (T_f), where almost all solutes are insoluble in ice. Secondly, the solidification (vitrification) of the remaining solution at the glass transition temperature (T_g'). Typically, ice grows as planar dendrites, thereby expelling most of the dissolved excipients (with a few exceptions). As a result, excipients become progressively concentrated and remain in a freeze-concentrated solution (FCS), both in between the ice dendrites (FCS₁) and outside the ice dendrites (FCS₂) [77]. The former event is called microscopic cryoconcentration and leads to FCS₁ distributed in between ice dendrites [78] (see Fig. 1A). The latter event is called macroscopic cryoconcentration and leads to FCS₂ distributed in a network of veins (see Fig. 1B). After the crystallization process of ice is complete, FCS still remains liquid until the whole solution is cooled below T_g' , or, in the presence of two different concentrations of FCS, below $T_{g,1}'$ and $T_{g,2}'$. Both the cooling rate and the nucleation temperature of ice have an impact on the size and the number of ice crystals formed during freezing [78,79]. Additionally, some of the cryoprotectants have an impact on the morphology of ice crystals and/or on the interaction of the solutes with surfaces such as ice itself or container walls. Other cryoprotectants act as buffers, antioxidants (prevent oxidation of protein), increase the surface tension of the solution or change the glass transition, freezing and melting temperatures of the solution (see Table 2). As mentioned earlier, there are excipients that are more likely to crystallize than others. Excipient crystallization can happen during cooling, storage and/or heating depending on the pH [18], composition of formulation [29,72,80] and cooling/heating rates [72]. In other words, whether an excipient crystallizes or remains amorphous is conditional on a specific formulation and FT process.

In this study, we investigate the impact of cryoprotectants on the freezing and thawing behavior of sodium citrate buffer. A citrate buffer was chosen since it is commonly applied in the formulation of biopharmaceuticals, especially in antibody formulations, showing a very low pH-shift in the frozen state [81]. Specifically, we look into their impact on ice dendrite orientation, ice platelet morphology, glass transition and melting temperatures. [78]

2. Material and methods

2.1. Sample preparation

25 mM sodium citrate buffers (pH 6.5) and 25 mM sodium citrate buffers with various cryoprotectants as listed in Table 2 were used.

2.2. Optical cryomicroscopy (OCM) measurements:

Measurements were done as described in our earlier work in reference [64] and reference [17]. In short, images of sample droplets containing buffer solution with added cryoprotectants were investigated using an optical microscope BX-51 (Olympus Corporation, Japan). Droplets (approximately 0.5 μ l in volume) were placed on a microscopy slide, which is temperature controlled by a Linkam cryostage LTS420 (Linkam Scientific Instruments, UK). Videos were recorded upon cooling to -80 °C and reheating to room temperature at various rates. Images were taken using standard transmitted light with or without a crossed-polarized filter.

2.3. Differential Scanning Calorimetry (DSC) measurements

Measurements were done as described in our earlier work in reference [17]. In brief, about 30 mg of sample were loaded into an aluminum crucible and hermetically sealed with a lid at room temperature. The crucible was then loaded to the oven of the DSC 8000 device (Perkin-Elmer, USA), cooled to -80 °C at a cooling rate of 40 °C/min, equilibrated for 5 min at that temperature and reheated at 40 °C/min to 5 °C. DSC signals are proportional to temperature change rate, such that weak signals can only be resolved for fast rates. This cooling/heating cycle was repeated three times. For calibration of the DSC instrument recommended transitions in cyclopentane, cyclohexane, indium, and adamantane were used to ensure correct transformation temperature at subzero temperatures with accuracy ± 1 °C [82]. Sapphire was used to calibrate latent heat and change in heat capacity enabling an accuracy of ± 0.1 J/mol °C.

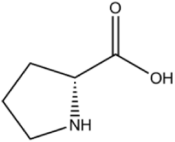
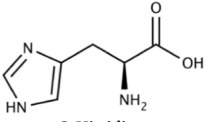
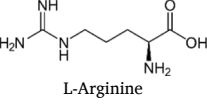
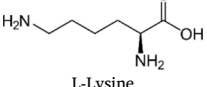
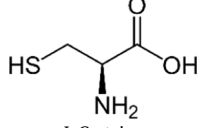
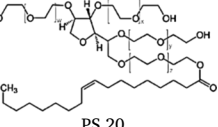
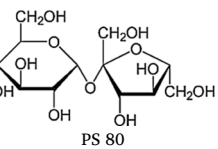
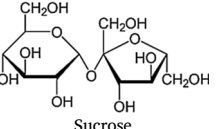
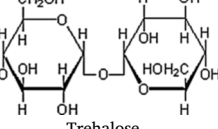
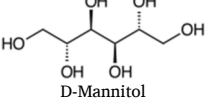
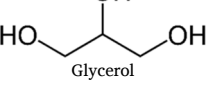
3. Results and discussion

3.1. Impact of cryoprotectants on the orientation of ice dendrites upon freezing

Fig. 2 and Fig. 3 show the OCM images of single droplets of water and solutions at -80 °C after cooling between 0.5 and 40 °C/min. The images in Fig. 2 were recorded in transmitted light, the images in Fig. 3 were recorded through crossed-polarizers to allow for better observation of individual crystallites. It is obvious that there are several changes on the morphology depending on both the cryoprotectant and the cooling rate. Pure Milli-Q water results in well-defined crystals that have sharp edges. Ice formation has clearly started from several nucleation sites within the droplet, and the crystal front has grown towards the diameter of the droplet. The lower the cooling rate the fewer nucleation sites, which ultimately leads to larger individual crystals within the droplet. Even without using a crossed-polarized filter, the direction of ice growth and orientation is clearly visible. Very similar findings apply for frozen sodium citrate buffer. Higher cooling rates result in smaller crystals and a more homogeneous distribution of ice within the droplet. This finding is rather general and applies to all cryoprotectant solutions studied here. However, the nucleation temperature of ice is barely affected by the choice of cooling rate. In most experiments, the first signs of ice are observed at about -30 ± 2 °C using OCM, no matter whether a cooling rate of 1 °C/min or 40 °C/min was used. The influence of cryoprotectants on the nucleation temperature is quite small, where histidine, lysine, PS20 and PS80 shift it slightly up to -25 ± 3 °C and sucrose and trehalose shift it slightly down to -35 ± 4 °C. In most cases the many nucleation sites lead to a fluffy and feathery appearance of the crystals

Table 1

Investigated additives with their cryoprotective properties/mechanisms and information about their natural occurrence (when applicable) and application as a cryoprotectant.

Cryoprotectant	Properties/Mechanisms	Occurrence/Deployment	Source
<p>Amino acids</p>  <p>L-Proline</p>	<ul style="list-style-type: none"> -osmoprotectant -antioxidant -reduces the excessive reactive oxygen species -binds to protein -ability to buffer 	<p><i>In nature:</i> Plants, yeast, fruit fly larva</p> <p><i>Artificially:</i> Oocyte vitrification, stem cells, ram sperm</p>	[35–42]
 <p>L-Histidine</p>	<ul style="list-style-type: none"> -ability to buffer (pH range 5–7) -non-crystallizing protein stabilizer -possesses both basicity and π-electron acceptor capability -forms strong complexes with metal ions and salts -antioxidant 	<p><i>In nature:</i> <i>n.a.</i></p> <p><i>Artificially:</i> Lyophilization</p>	[43–46]
 <p>L-Arginine</p>	<ul style="list-style-type: none"> -improves refolding efficiency -suppresses protein aggregation and protein–protein or protein–surface interactions -increases the surface tension of water -increases solubility of native protein states -carboxylated poly L-Lysine inhibits the formation and recrystallization of intracellular ice -strong hydrogen bond interactions of interstitial water molecules 	<p><i>In nature:</i> Yeast, larvae, fish</p> <p><i>Artificially:</i> Spray-Drying</p>	[47–50]
 <p>L-Lysine</p>	<ul style="list-style-type: none"> -carboxylated poly L-Lysine inhibits the formation and recrystallization of intracellular ice -strong hydrogen bond interactions of interstitial water molecules -prevents water from forming crystalline seeds -reducing agent -antioxidant -increases post-thaw motility and viability 	<p><i>Artificially:</i> Spray-Drying</p>	[51–55]
 <p>L-Cysteine</p>	<ul style="list-style-type: none"> -prevents water from forming crystalline seeds -reducing agent -antioxidant -increases post-thaw motility and viability 	<p><i>In nature:</i> Insects + microalga in combination with antifreeze-proteins</p> <p><i>Artificially:</i> Buffalo semen, oocytes cryopreservation, ram spermatozoa</p>	[56–59]
<p>Surfactants</p>  <p>PS 20</p>	<ul style="list-style-type: none"> -reduces formation of insoluble aggregates -competes with stress-induced soluble aggregates for interfaces -surface-active -amphipathic and non-ionic -undergo auto-oxidation -known for chemical and enzymatic hydrolysis 	<p><i>Artificially:</i> Frozen foods, therapeutics, pharmaceuticals</p>	[60–63]
 <p>PS 80</p>	<ul style="list-style-type: none"> -prevents surface adsorption of protein -protein stabilizer -surface-active -amphipathic and non-ionic -reduces interfacial stress -undergoes auto-oxidation -known for chemical and enzymatic hydrolysis 	<p><i>Artificially:</i> Frozen foods, therapeutics, pharmaceuticals, emulsions</p>	[61–64]
<p>Disaccharide</p>  <p>Sucrose</p>	<ul style="list-style-type: none"> -as osmolyte reduces the loss of cellular water -inhibits (cold-)crystallization -stabilizes conformation of protein 	<p><i>In nature:</i> Plants</p> <p><i>Artificially:</i> Liposomal delivery systems</p>	[17,44,65–67]
 <p>Trehalose</p>	<ul style="list-style-type: none"> -stabilizes macromolecules via direct interaction with hydration shell -stabilizes conformation of protein 	<p><i>In nature:</i> Larvae, insects</p> <p><i>Artificially:</i> Liposomal delivery systems</p>	[67–70]
<p>Polyhydric alcohols</p>  <p>D-Mannitol</p>	<ul style="list-style-type: none"> -reduces the loss of cellular water as osmolyte -inert -good cake supporting properties 	<p><i>In nature:</i> Yeast</p> <p><i>Artificially:</i> Lyophilization</p>	[65,66,71,72]
 <p>Glycerol</p>	<ul style="list-style-type: none"> -lowers the freezing point -prevents freezing of intra- and extracellular fluid -binds to protein, -stabilizes hydration shell around protein -increases 'bound' water -reduces extracellular ice formation/dehydration -reduces the loss of cellular water as osmolyte 	<p><i>In nature:</i> Insects, yeast, fish</p> <p><i>Artificially:</i> Food, car, pharmaceutical, medical industries</p>	[38,41,65,73–76]

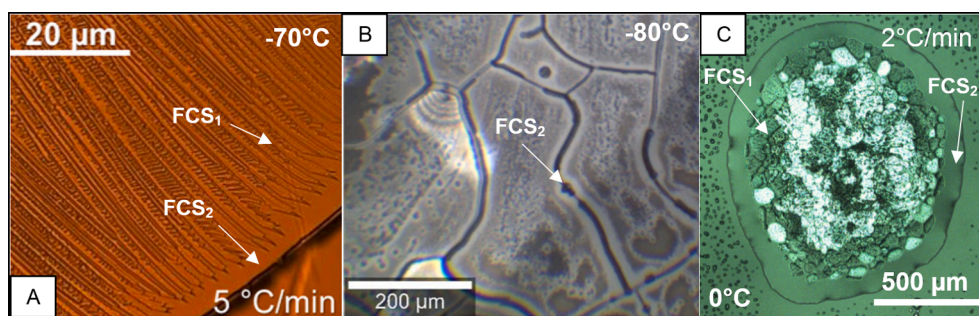


Fig. 1. OCM images of (A) 25 mM sodium citrate buffer at -70°C , (B) monoclonal antibody solution at -80°C and (C) 25 mM sodium citrate buffer at 0°C during melting. Images A + B taken from reference [78]. Note the different length scale!

Table 2

List of cryoprotectants and their concentration in solutions.

	Cryoprotectant	Concentration	Manufacturer	CAS No.	Purity	pH*
Sodium citrate		25 mM	Sigma-Aldrich	6132-04-3	$\geq 99.5\%$	6.5
+						
Amino acids	L-Proline	100 mM	Sigma-Aldrich	147-85-3	$>99.5\%$	6.5
	L-Histidine	100 mM	Sigma-Aldrich	71-00-1	$>99.5\%$	7.5
	L-Arginine hydrochloride	100 mM	Sigma-Aldrich	1119-34-2	$>98\%$	6.3
	L-Lysine hydrochloride	100 mM	Sigma-Aldrich	657-27-2	$>99.5\%$	6.3
	L-Cysteine	100 mM	Sigma-Aldrich	52-90-4	$>99.5\%$	6.4
Surfactants	Polysorbate 20	0.4 wt%	Sigma-Aldrich	9005-64-5	n.a.	6.5
	Polysorbate 80	0.4 wt%	Sigma-Aldrich	9005-65-6	n.a.	6.5
Sugars	Sucrose	100 mM	Sigma-Aldrich	57-50-1	$>99.5\%$	6.5
	Trehalose dihydrate	100 mM	Sigma-Aldrich	6138-23-4	$>99\%$	6.5
Polyhydric alcohols	D-Mannitol	100 mM	Merck	69-65-8	$>99.7\%$	6.5
	Glycerol	0.4 wt%	Fluka	56-81-5	$>99.5\%$	6.5

* pH value was determined at 22°C – 25°C with a conventional pH electrode

within the droplet at $40^{\circ}\text{C}/\text{min}$.

The most differences are found for the low cooling rates that are of greater importance for the freezing of large-scale solutions. Addition of arginine for instance leads to homogeneous freezing even for cooling rates of $0.5^{\circ}\text{C}/\text{min}$. This is easy to see in Fig. 3, which does not feature large oriented crystals, but much smaller randomly oriented crystals. That is, arginine has the ability to initiate freezing at many locations within the droplet and sterically hinder formation of long branches. At higher cooling rates, a rim around the droplets diameter appears. This indicates that in addition to the freezing of the droplet from inside out, at later stages also freezing from the outside sets in. Such a ring also forms in case of lysine, but not for other cryoprotectants. Lysine also results in less sharp edges and more wavy crystals, featuring a smooth transition of shades of green. Some cryoprotectants, such as cysteine cause dehydration of the droplet and favor crystallization of excipients. These excipient crystals show brighter features in the OCM at -80°C in Fig. 2 and darker features in Fig. 3, where ice dendrites appear as long needles. Proline and histidine on the other hand have the ability to limit the proliferation of ice dendrites – this is evidenced through microscopy images reminiscent of the dimple pattern of a golf ball. Only at the highest cooling rate, namely $40^{\circ}\text{C}/\text{min}$, this freezing pattern is compromised. The black dots in the OCM image might indicate sodium citrate-histidine clusters, where histidine is known for its ability to form complexes with ions (see Table 1). Self-aggregation is, however, absent for histidine. This clustering then also hinders proliferation of ice crystals. Some of the droplets do not show any ice crystal formation but rather appear transparent (see Fig. 4). This effect can be traced back to the osmoprotectant properties of proline which limits ice growth and favors vitrification [83] resulting in a glassy solid at -80°C . By contrast, the disaccharide trehalose yields dendritic growth originating from a single nucleation site within the droplet. Star-like growth towards the perimeter is evident in Figs. 2 and 3. Additionally, long dark crystal structures (standard-transmitted light) assigned to formation of the

cryo-protectant hydrate, namely trehalose dihydrate, appear. High cooling rates seem to induce development of small ice platelets that are not interconnected. This is similar for sucrose at least at low cooling rates, providing ample time for the FCS to remain in the liquid state before it vitrifies (at T_g'). Also for mannitol star-like patterns are readily identified at rates of 0.5 – $1^{\circ}\text{C}/\text{min}$ in Fig. 3. From these star-like patterns fine lines lead to the perimeter of the droplet. Ice dendrites disappear for a rate of $2^{\circ}\text{C}/\text{min}$. Instead, the droplet seems to be full of thin needles indicating crystallization of mannitol hydrate. A further increase of cooling rate results in the appearance of larger ice dendrites, similar to sodium citrate buffer cooled at $40^{\circ}\text{C}/\text{min}$.

The surface-active surfactants polysorbate 20 and polysorbate 80 show grainy, rough surfaces with white spots at low cooling rates (see Fig. 2), but smoother surfaces above $10^{\circ}\text{C}/\text{min}$ without white spots. This suggests that the surfactants favor the formation of large ice dendrites. We assume that this is related to the slightly higher nucleation temperature (see above). In fact, none of the droplets provides clues to the initial nucleation sites, i.e., crystal growth starts simultaneously at many well-distributed spots. This is similar for glycerol, where the ice dendrites are smaller and the edges are more rugged. At a cooling rate of $0.5^{\circ}\text{C}/\text{min}$, a homogenous distribution of FCS and/or a total coverage of ice surface appears. The white dots (Fig. 2) noticed for PS20 and PS80, are absent. Yet, the black spots seen at $40^{\circ}\text{C}/\text{min}$ are present in glycerol and surfactant solutions. That is, the black dots are presumably crystalline citrate buffer. This would mean that there is a tendency of citrate crystallization when higher cooling rates are applied.

3.2. Impact of cryoprotectants on the glass transition and initial melting temperature

The glass transition temperatures of the freeze-concentrated solutions (T_g' s) were determined using differential scanning calorimetry (DSC). Since the optical appearance does not change at T_g' , DSC

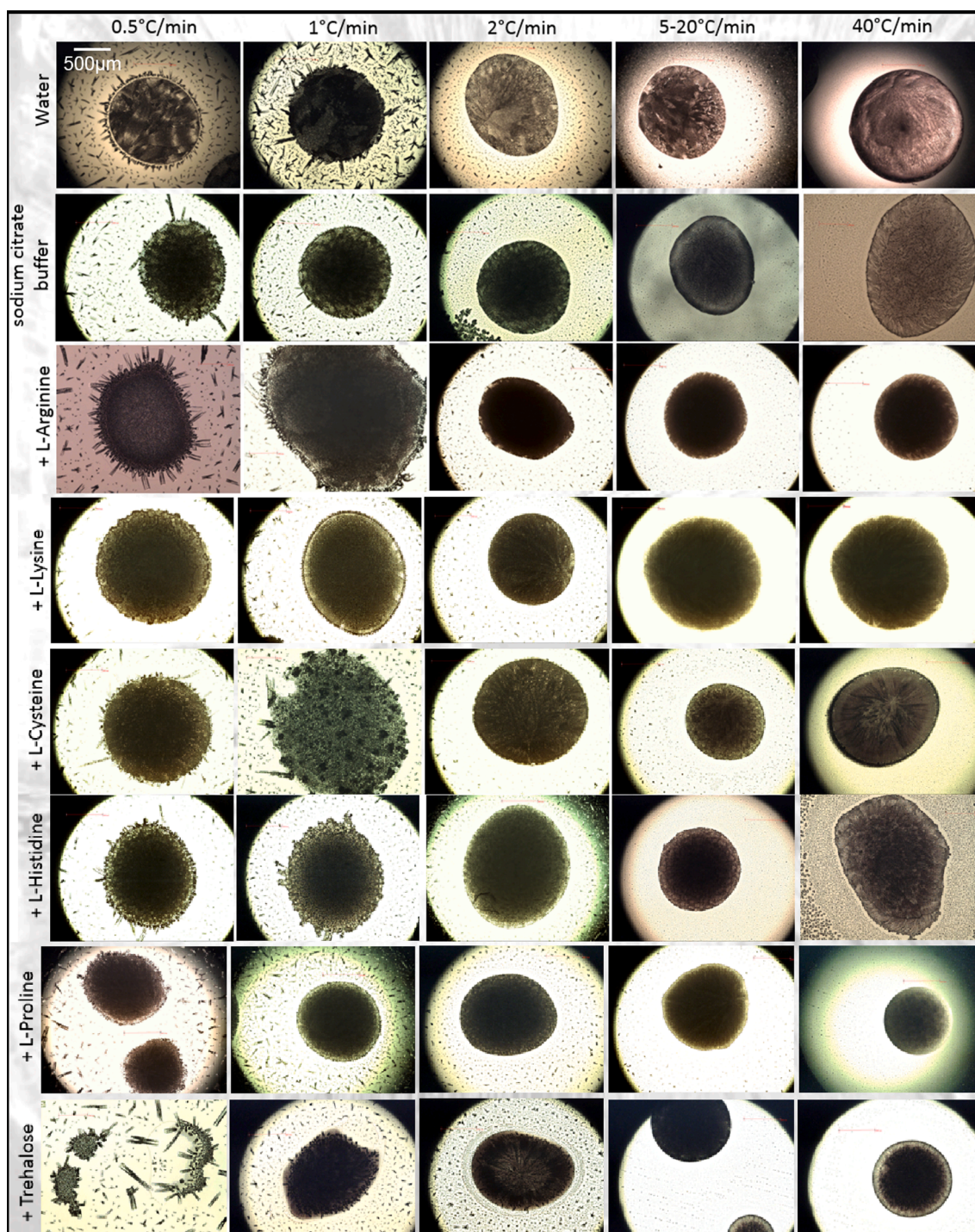


Fig. 2. OCM images of water and 25 mM sodium citrate buffer with or without cryoprotectants at $-80\text{ }^{\circ}\text{C}$ after applying various cooling rates. Images are taken with standard transmission light.

measurements are needed to determine T_g' (see Fig. 5). The tangent evaluation method [84] was used to extract T_g' from each heating scan (see Supplementary Material). After freezing the sample volume consists of about 99% pure ice and 1% freeze-concentrated solution. Since T_g' pertains to the freeze-concentrated solution a very high instrument sensitivity is required to detect it. Furthermore, the DSC signal is proportional to the heating rate used for scanning, i.e., high rates produce larger signals. However, high rates increase thermal lag and cause difficulties in determining accurate temperatures. As a compromise, we

have used scanning rates of $40\text{ }^{\circ}\text{C}/\text{min}$, which allow detecting the subtle glass transition features and still allowing for a precision for T_g' of better than $\pm 3\text{ }^{\circ}\text{C}$. All T_g' 's extracted using this procedure are summarized in Fig. 6 to ease comparability.

Sodium citrate buffer solutions without cryoprotectant show two glass transitions at $-51\text{ }^{\circ}\text{C}$ and $-41\text{ }^{\circ}\text{C}$ upon heating (indicated by red ellipse around data points in Fig. 6). Generally, the presence of two T_g' 's in aqueous solutions is a common observation and is attributed to the presence of two different concentrations of FCS within the droplet [85].

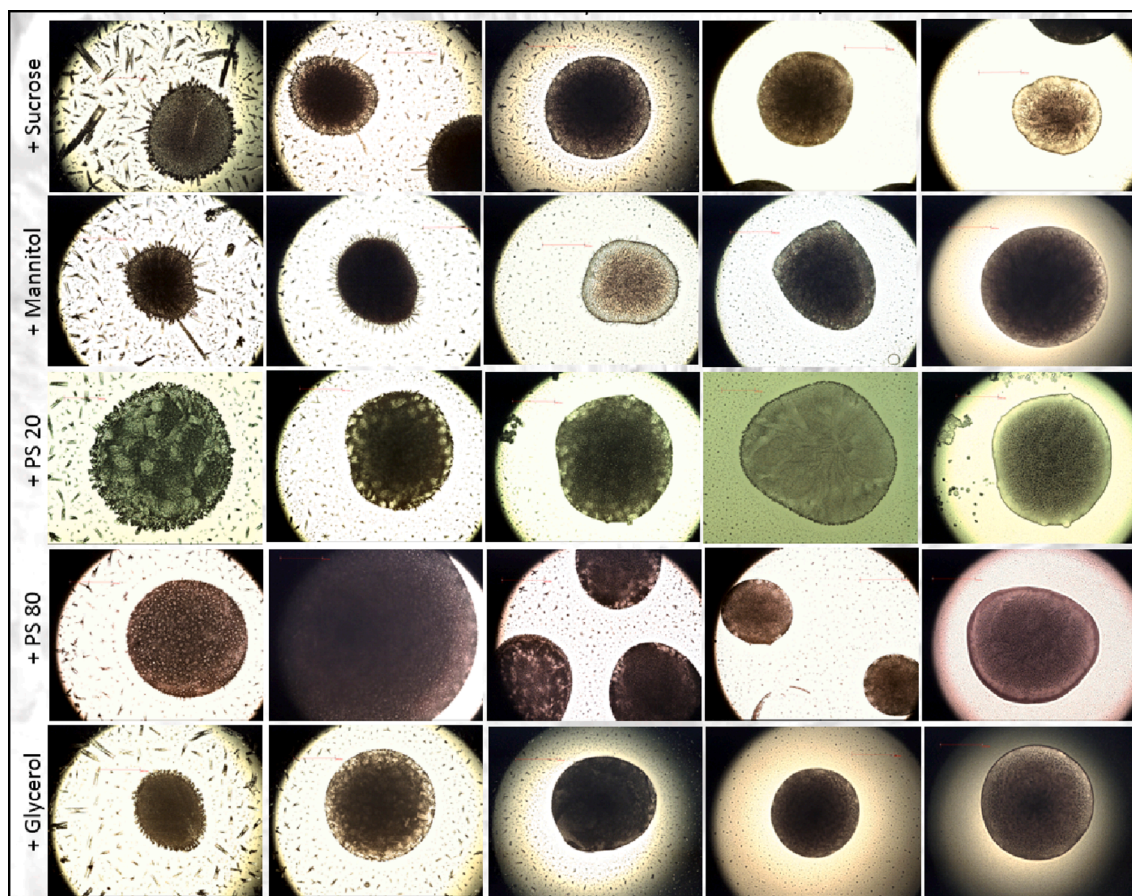


Fig. 2. (continued).

One type of FCS is trapped in between the ice crystals in the interior of the droplet, the second type is pushed outwards to the diameter of the droplet by the growing ice front. The thermograms change after adding 100 mM or 0.4 wt% cryoprotectant, except for cysteine. Histidine, sucrose and trehalose (all marked with blue ellipses in Fig. 6) also show two T_g 's, where both of them are shifted to higher temperatures.

The two T_g 's of histidine both show a temperature shift of +4.5 °C, to –46.5 °C and –36.5 °C, respectively. That is, there is a plasticizing effect of histidine on the freeze-concentrated solution. In previous studies by Österberg and Wadsten, histidine solution was reported to have a single T_g ' value of –32 °C [44,86] at pH 6 and –35.4 °C at pH 6.5 [44] which is the pH value of our solutions. They justify the pH dependent T_g shift with the plasticizing effect of buffer ions present in solution. While the second T_g ' reported by Österberg and Wadsten is in very good agreement with ours, they do not report the lower T_g ', probably because a very high sensitivity is necessary to detect it. As seen in Fig. 5 the T_g ' at –46.5 °C is much feebleness than the one at –36.5 °C. Since the two T_g 's seen in pure sodium citrate buffer shift equally to higher temperatures after adding histidine (without changing the pH value), the formation of complexes with the buffer salt might cause the shift of both T_g 's.

Both T_g 's are upshifted also for sucrose and trehalose. The T_g ' at higher temperature shifts by 9° and 12 °C to –32 °C and –29 °C compared to the cryoprotectant-free solution, respectively. These high values are very well known and typical for those disaccharides [17,87]. The lesser-known lower T_g ' at –44 °C and –43 °C is indicative of FCS with a concentration close to the maximal freeze-concentration within the droplet. The sucrose-water state diagram shows the correlation of concentration and T_g ' [88]. According to this diagram our T_g 's indicate two FCS with different concentrations within the droplet, one FCS with almost 80 wt% sucrose (FCS₂, lower T_g ') and another FCS with a slightly

different concentration of sucrose (FCS₁, higher T_g '). The same assumption applies for trehalose, taking into consideration that trehalose, as reported in literature, exhibits higher T_g 's compared to sucrose with the same concentration [89–91]. The high glass transitions temperatures of freeze-concentrated sucrose and trehalose solutions derive from the fact that sugars have many hydroxyl groups which form hydrogen bonds with ice [92] thereby increasing viscosity. In addition, this hydrogen-bonding ability of sugars also suppresses (cold-) crystallization.

Also mannitol solutions are marked by a blue ellipse in Fig. 6 since they exhibit two T_g 's at –52 °C and –37 °C. However, by contrast to the cryoprotectants mentioned above a crystallization event at –18 °C dominates the heating scan in Fig. 5. This crystallization event is preceded by a weak endothermic event at –25 °C. In literature two T_g 's in aqueous mannitol solutions at –32 °C and –25 °C and the crystallization of mannitol hydrate are reported [72]. In that study, Cavatur and co-workers detected a T_g ' in mannitol/phosphate buffer solutions at –38 °C just prior to crystallization of the buffer salt [72]. Additionally, in other studies, T_g ' of maximally FCS of mannitol solutions is around –30 °C [93,94]. Different from Ref. [72] we assign the endothermic increase at –25 °C as the onset of eutectic melting. A similar endothermic increase takes place for all other solutions shown here in Fig. 5, which ends in eutectic melting. Only in mannitol solutions the eutectic melting event is interrupted by cold-crystallization.

The amino acid arginine and the surfactants PS20 and PS80 just display one T_g ' at –44 ± 1 °C (see Fig. 6, marked by green rectangles). Similarly, solutions containing glycerol, lysine and proline show one T_g ' at –54 ± 1 °C (see Fig. 6, marked by yellow rectangles). That is, for the former three cases the T_g ' is just below the higher T_g ' of the sodium citrate solution. By contrast, for the latter three cases, it is just below the

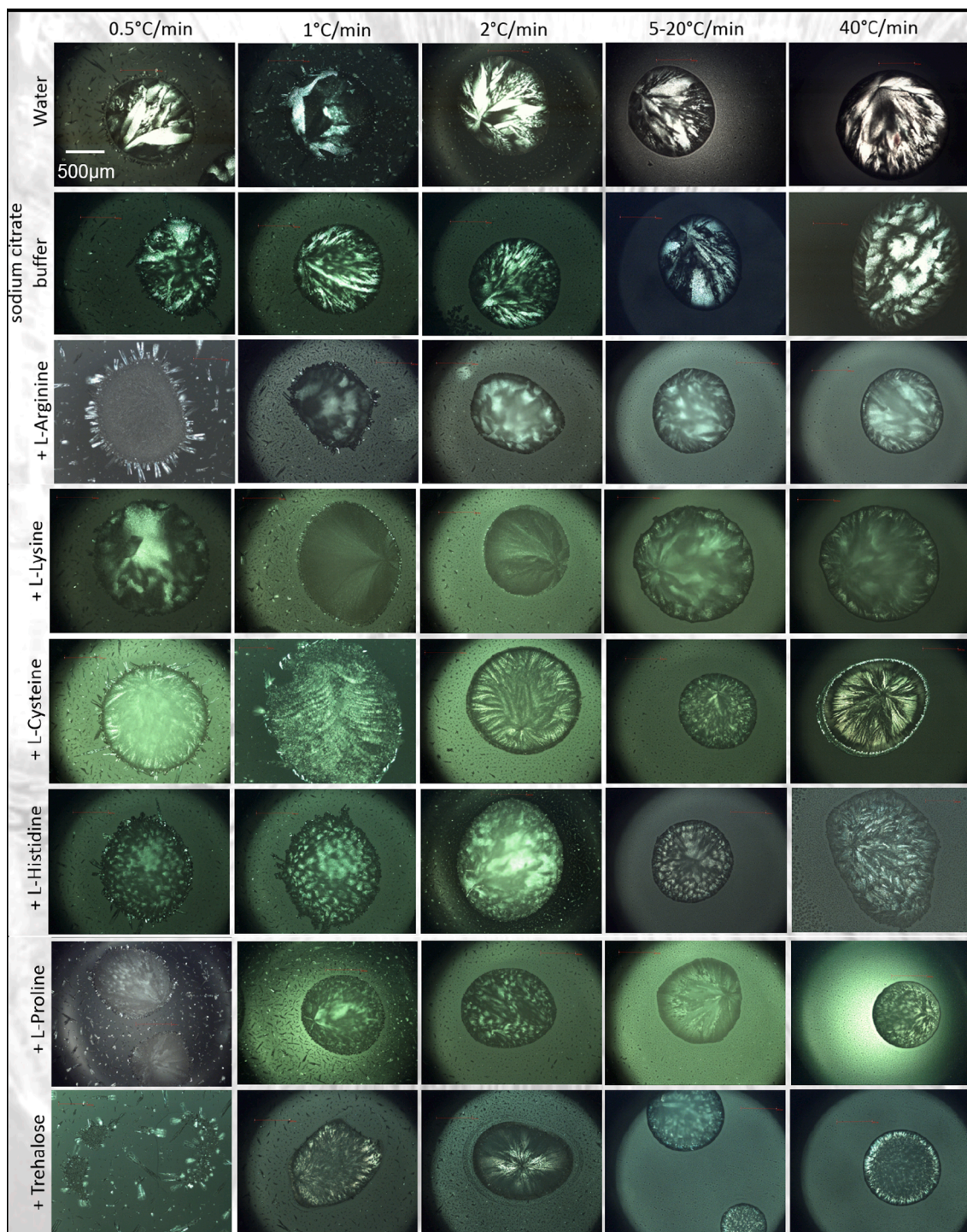


Fig. 3. OCM images of water and 25 mM sodium citrate buffer with or without cryoprotectants at $-80\text{ }^{\circ}\text{C}$ after applying various cooling rates. Images are taken with a crossed-polarization filter.

lower T_g' of the sodium citrate solution. Generally, the disappearance or predominance of a single glass transition indicates the presence of just one concentration of FCS within the droplet (or a very small amount of the second concentration, which falls below the detection limit of the instrument). Apparently, these six solutions avoid the formation of FCS₁ and FCS₂, where arginine, PS20 and PS80 produce FCS₁, but glycerol, lysine and proline produce FCS₂.

Fig. 7 focuses on the initial melting temperature $T_{m,i}$, as determined both from DSC and OCM. OCM images taken during heating are in the

Supplementary Material. Using OCM, $T_{m,i}$ is defined as the temperature at which mobility sets in within the droplet, hence, the first ice crystals start melting. $T_{m,i}$ was averaged for all heating rates from $0.5\text{ }^{\circ}\text{C}/\text{min}$ to $40\text{ }^{\circ}\text{C}/\text{min}$. Using DSC $T_{m,i}$ is defined as the point within the thermogram where the baseline starts deviating (see **Fig. 7A**). $T_{m,i}$ s from both methods are summarized in **Fig. 7B** and **Fig. 7C**.

Glycerol, lysine and proline have the lowest initial melting temperatures ($T_{m,i}$) – and, the lowest freezing temperature. Those three substances seem to suppress the ice crystal formation and growth. By

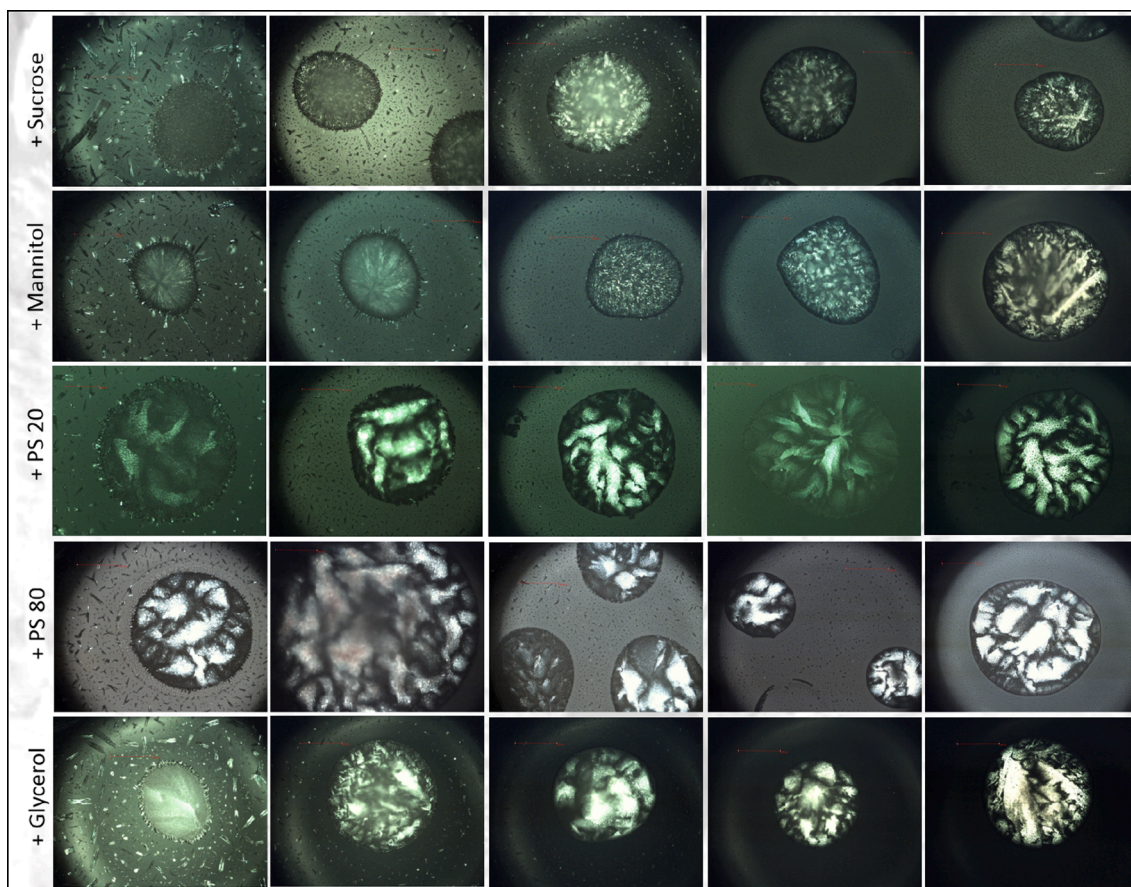


Fig. 3. (continued).

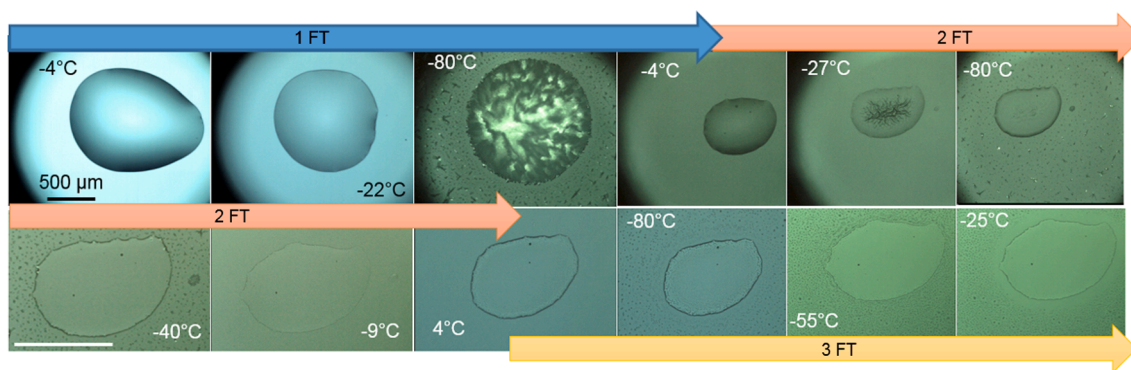


Fig. 4. OCM images of sodium citrate buffer with 100 mM proline during repeated FT-cycles to the set-point temperature of $-80\text{ }^{\circ}\text{C}$ for three times. The lower row of images shows the droplet with a twice as high magnification (bar indicates $500\text{ }\mu\text{m}$).

suppressing ice crystal growth and preventing dehydration, higher unfrozen water content may stay outside of the ice crystals [83] defined as FCS_2 . Following this assumption, this would mean that those three cryoprotectants have a plasticizing effect on sodium citrate solution due to the higher unfrozen water content. Consequently, FCS_2 features higher mobility, which results in a lower T_g' . The cryoprotectants arginine, PS20 and PS 80 are known to be surface-active, whether it is with the protein in therapeutic formulations ice dendritic surfaces [95] or container surfaces. This interaction with various surfaces could be a reason for the late devitrification of the glassy FCS within the droplet and the higher T_g' . Sodium citrate buffer shows a $T_{m,i}$ of $-15\text{ }^{\circ}\text{C}$ (OCM) and $-20\text{ }^{\circ}\text{C}$ (DSC). By adding the cryoprotectants trehalose, sucrose, PS80, PS20, mannitol, histidine and cysteine a trend of a $T_{m,i}$ -shift to

higher temperatures is observed, at least in DSC measurements. In OCM measurements the $T_{m,i}$ is found at $-15 \pm 2\text{ }^{\circ}\text{C}$ for this subset of cryoprotectants, except for PS20. By contrast, proline, arginine, lysine or glycerol show lower $T_{m,i}$, namely between $-21\text{ }^{\circ}\text{C}$ and $-31\text{ }^{\circ}\text{C}$ in OCM measurements. In DSC measurements, this effect mainly shows for glycerol and lysine. The differences between the DSC and OCM measurements are illustrated best in the bar diagram in Fig. 7B, where especially proline deviates significantly in the two methods. In spite of these inconsistencies, it appears that the cryoprotectants can be divided into three groups depending on the impact they have on $T_{m,i}$.

Group 1 (PS20, PS80, histidine or arginine) contains the cryoprotectants that barely (or inconsistently) impact $T_{m,i}$. In general, $T_{m,i}$ changes when the concentration (or more precisely, activity) of the FCS

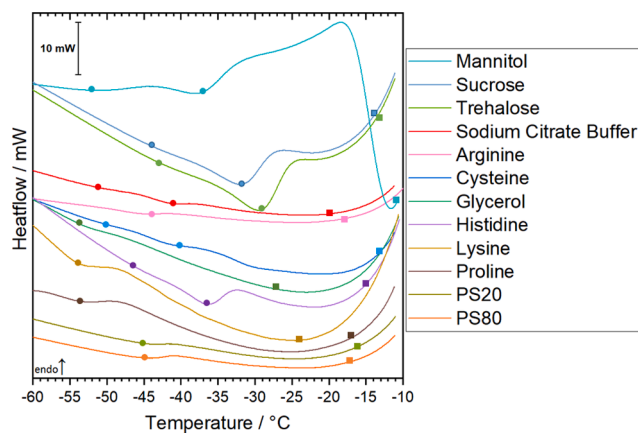


Fig. 5. DSC thermograms of sodium citrate buffer solutions with and without cryoprotectants, scanned at a heating rate of 40 °C/min. Circles represent T_g' and squares indicate the initial melting temperature ($T_{m,i}$). Linear baselines were subtracted from the raw data.

surrounding the ice crystals changes. Group 1 cryoprotectants do not cause significant changes in the activity of the FCS. Group 2 cryoprotectants (cysteine, trehalose, sucrose or mannitol), increase $T_{m,i}$, i.e., they lower the activity of the FCS. This might be achieved by attaching to the ice surface directly rather than staying inside the FCS. This mechanism also explains why disaccharides restrict ice dendritic growth: they simply block the ice growth sites through adsorption on the ice facets. This property may be an explanation for the delayed ice melting. Group 3 cryoprotectants (proline, lysine or glycerol) would then reduce $T_{m,i}$ by staying preferentially in the FCS, avoiding adsorption at the ice surface. By preferred binding to water in the liquid state they are also excellent ice inhibitors.

3.3. Impact of cryoprotectants on the morphology of ice platelets

OCM images of droplets taken just before complete melting, just before the droplet appears transparent, are reported in Fig. 8. Depending on heating rates this occurs at temperatures between -20 °C and -2 °C. In general, the higher the heating rate, the higher the temperature of complete melting. This reflects the time needed for the droplet to assimilate and adapt to the set temperature and to experience melting.

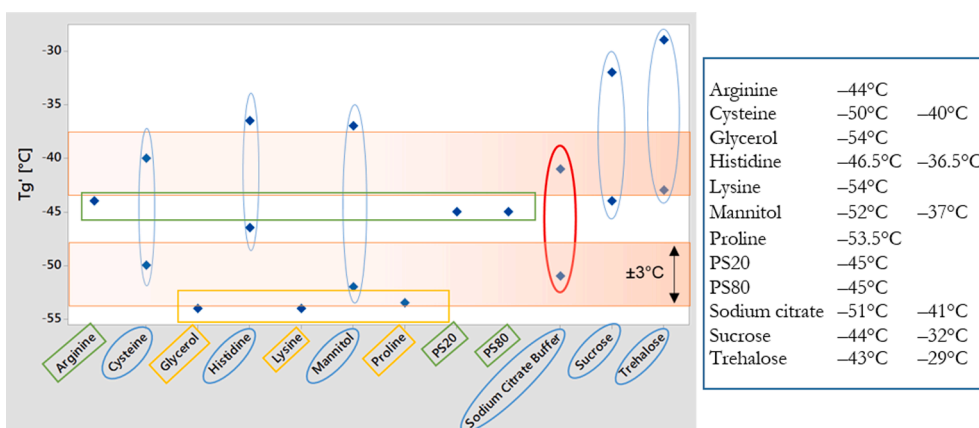


Fig. 6. Glass transition temperatures T_g' of solutions containing sodium citrate buffer with or without cryoprotectants. Ellipses around data points and names indicate solutions with two T_g' 's. Yellow and green rectangles indicate a single T_g' at -54 °C or -45 °C, respectively.

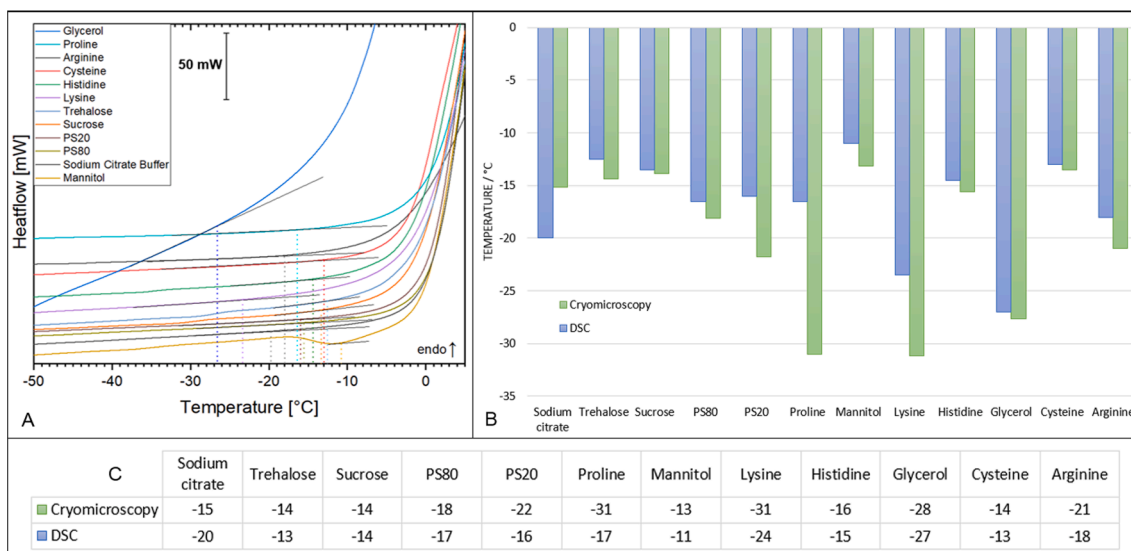


Fig. 7. (A) DSC thermograms of heating 25 mM sodium citrate buffer with or without 100 mM cryoprotectants at 40 °C/min. Please note that this is the same as Fig. 5, but with a smaller magnification, without baseline subtraction and a broader temperature range. (B) Bar diagram comparing $T_{m,i}$ determined by DSC and OCM. (C) Table with $T_{m,i}$ determined by both methods.

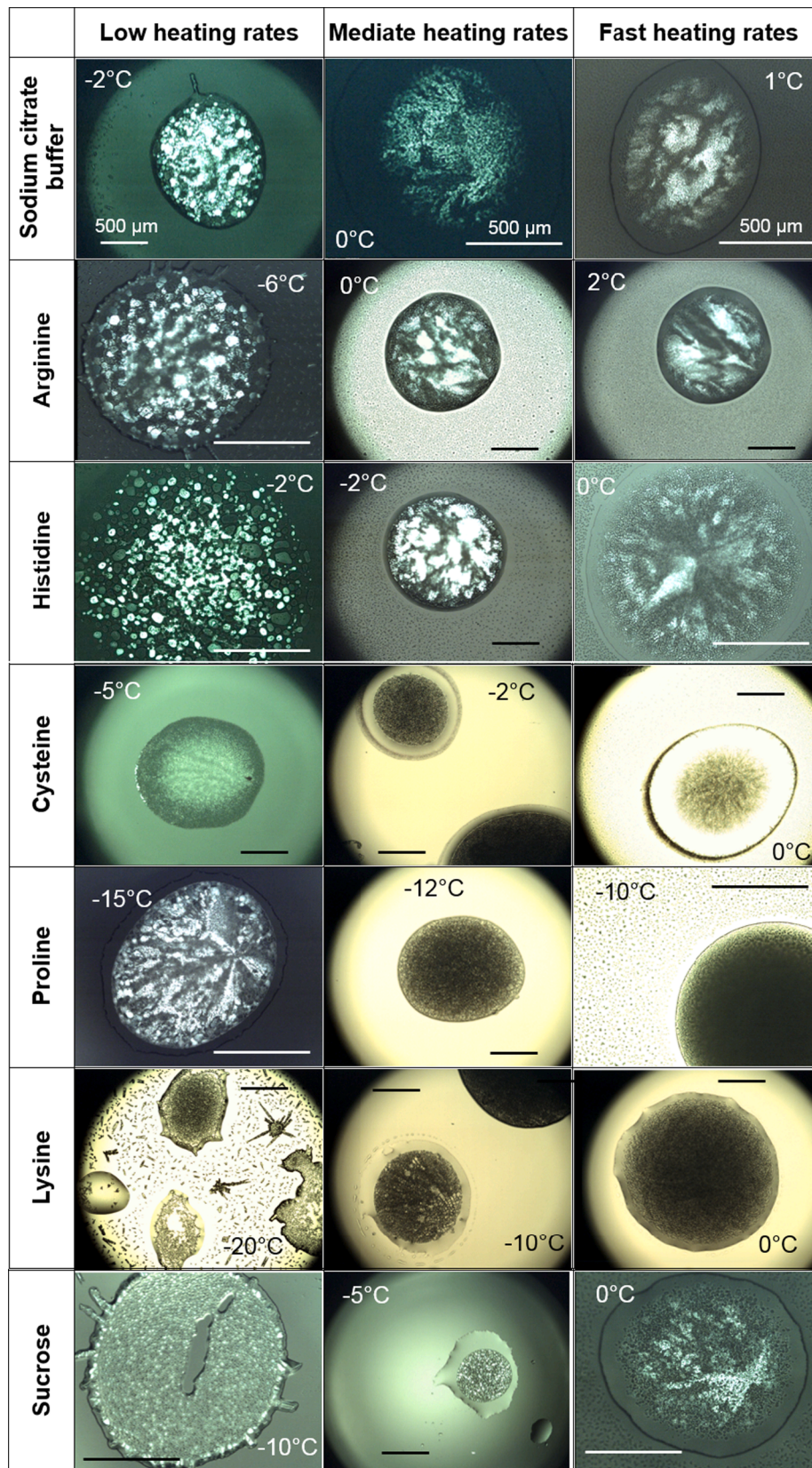


Fig. 8. OCM images of droplet containing 25 mM sodium citrate buffer without and with 100 mM cryoprotectant upon heating at various rates taken before complete melting (scale bar indicates 500 μm).

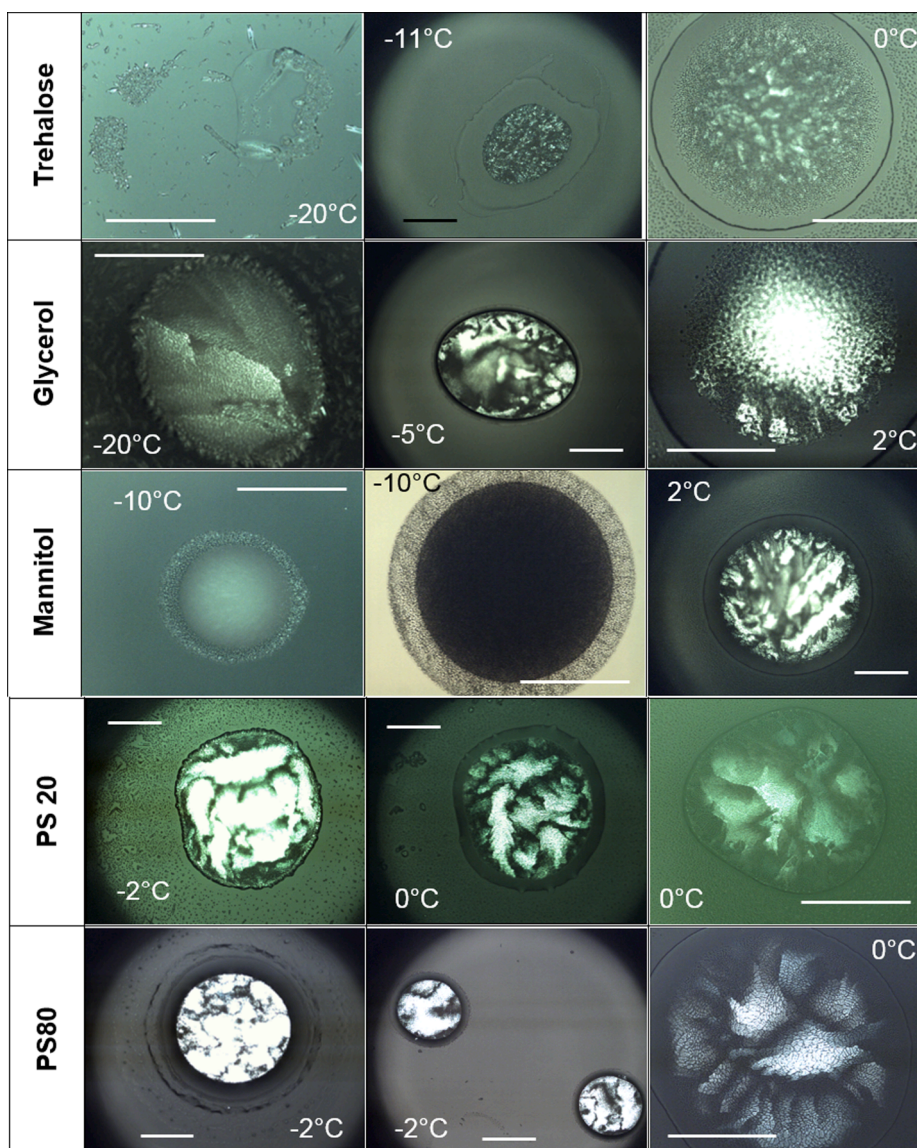


Fig. 8. (continued).

Addition of the cryoprotectants histidine and arginine to sodium citrate buffer does not seem to have an additional impact on the morphology of the ice platelets nor on the melting event of the solution. Differences show when adding the amino acid lysine, which appears to work like glue, holding together a meshwork of little chunks and crystals. Especially at low heating rates an atypical melting of the crystals in lysine solution can be noticed, i.e., melting is not only starting from the perimeter of the droplet and proceeding to the center but also starts at other spots of the droplet.

Compared to all other cryoprotectant solutions, round ice platelets are not present. This morphology supports the statement that lysine interacts strongly with liquid water, but less so with the ice crystals. Also upon cooling crystalline seeds are inhibited through the formation of strong hydrogen bonds with water molecules. Only one other amino acid shows similar effects in sodium citrate buffer, and this is proline. The effects of the osmoprotectant proline on the ice morphology within the droplet are highlighted in Fig. 4. This shows multiple freeze and thaw cycles, where proline acts like glue, forming a mycelium/meshwork that keeps the structures linked together (see image at -80°C in first cycle, and image at -27°C in second cycle). Furthermore, after several cycles the solid droplets at -80°C appear transparent, as expected for non-crystalline, vitrified water.

The amino acid cysteine and the polyhydric alcohol mannitol cause a dehydration of the droplet when applying low heating rates. As a result, a scaffold of dried/crystalline solution remains as a cake (see Fig. 8). At higher heating rates, a solution containing cysteine melts but a solid circle remains, designating where the borders of the droplet had been. In contrast, droplets containing mannitol do melt completely, excipients and buffer salt dissolve and a transparent droplet results. Mannitol is prone to crystallize at lower cooling and heating rates, which can be seen in images taken at -80° as well as in images upon complete melting (see Fig. 2, Fig. 3 and Fig. 8). The remaining structure of the droplet after melting can be explained by complete dehydration - which is not surprising since mannitol is known for the cake supporting properties during lyophilization. Higher cooling and heating rates (above $20^{\circ}\text{C}/\text{min}$) seem to prevent total dehydration of the droplet.

The second polyhydric alcohol glycerol shares similar properties with the two surface-active surfactants polysorbate 20 and polysorbate 80. All three have relatively low $T_{m,i}$ (glycerol being the lowest, see Fig. 7) but prevent shrinking of the frozen droplet until close to 0°C (see Fig. 8). In other words, solutions containing those cryoprotectants present the largest temperature range from initiation to complete melting. Effects like coverage of ice platelets with an oil film are observed in OCM images. No round ice crystals can be identified, rather more edgy ice

chunks surrounded by veins filled with FCS. Upon melting ice platelets do not move around, like usual, but are rather glued together and dragged towards the center of the droplet.

Both sugars trehalose and sucrose yield multiple small ice crystals. Interestingly, these small ice crystals do not share the same orientation, as evidenced by the different shades of green of platelets. The melting of droplets shows that sugars do inhibit the growth of ice crystals, which could be traced back to possible attachment to the ice surface [92]. The roundly shaped crystals do not move around during melting, but are stabilized above the glass transition by sugars.

4. Conclusion

In our study we investigated the impact of cryoprotectants on the morphology of ice crystals and on the glass transition and initial melting temperature in sodium citrate buffer. Depending on the cryoprotectant and on the cooling rate the morphology and the orientation of ice dendrites change. The frozen droplets at $-80\text{ }^{\circ}\text{C}$ in pure buffer solution, without any cryoprotectants, exhibit sharp edges, indicating an unconstrained ice growth in the droplet. Addition of PS20, PS80 and glycerol causes an increase of ice crystal size contrary to mannitol, sucrose, histidine and proline, which show a tendency of suppressing ice dendritic growth. Additionally, at lower cooling rates droplets containing disaccharides do not show any individual ice crystals (at the μm -resolution of our microscope), giving the appearance of homogeneous distribution of FCS without any detectable ice dendrite borders. Arginine and lysine soften the ice borders and give the droplet a cloudy appearance. Cysteine, trehalose and partially mannitol (at lower cooling rates) seem to disturb ice dendritic growth, as inferred from rays originating from several spots within the droplet or the barbules of a feather.

How these different ice morphologies affect the glass transition temperatures (T_g') and initial melting temperatures ($T_{m,i}$) is summarized in Fig. 5 and Fig. 7, respectively. The overall picture obtained in this work is presented in the Scheme in Fig. 9. Cysteine, mannitol, histidine, sucrose and trehalose, like pure sodium citrate buffer, show two T_g' 's. Most of the cryoprotectants, though, lead to the prevalence of only one T_g' when added to the buffer solution. Arginine, PS20 and PS80 exhibit only the higher T_g' and glycerol, lysine and proline feature the lower T_g' . The occurrence of just one T_g' implies the presence of only one predominant FCS within the droplet. Mannitol, being the exception, shows a cold-crystallization event to mannitol hydrate in addition to the two T_g' 's. In other words, the choice of cryoprotectant allows governing whether macroscopic or microscopic cryoconcentration dominates, or whether both processes take place simultaneously upon freezing. As a result, there are either two different FCS solutions differing in terms of

concentrations, or only one uniform FCS. Depending on the type of protein to be protected from aggregation either of the three possibilities might be beneficial – so that our work offers three different choices for cryoprotectants that lead to three different physical mechanisms of cryoprotection.

Also concerning $T_{m,i}$ cryoprotectants can be categorized into three groups depending on whether they raise, lower or do not have any impact on $T_{m,i}$ compared to pure sodium citrate buffer. The cryoprotectants that do not change $T_{m,i}$ are PS20, PS80, histidine, and arginine. Cysteine, trehalose, sucrose and mannitol raise $T_{m,i}$ to higher temperatures which may be explained by a reduced activity of the FCS and preferential adsorption on the ice surface. This also affects ice dendritic growth, where disaccharides restrict dendritic growth efficiently. The earlier start of melting by addition of proline, lysine or glycerol may be traced back to the strong interaction of cryoprotectant with the unfrozen water in the FCS. Similar conclusions have been reached in earlier work, where cryoprotectants were shown to prevent water from crystallizing due to strong hydrogen bonding interactions of the water molecules in the liquid [83,96].

The ice crystal morphology is not affected by histidine and arginine. Cysteine and mannitol cause dehydration of the entire droplet when low heating rates are applied. Droplets containing lysine and proline melt at various points within the droplet and act like glue holding the ice crystals together. Droplets containing PS20, PS80 and glycerol show big ice crystals; in contrast to droplets containing sucrose and trehalose, which present significantly smaller ice crystals indicating that those disaccharides limit ice crystal growth.

Each of our cryoprotectants has different properties; hence, in order to make best use they have to be chosen in the context of transport and storage temperature of the final protein solution. Regarding stability of the solution, storage below T_g' of the formulation is recommended but not absolutely necessary. On that point we want to emphasize that the optimal storage temperature is highly dependent on protein formulation (including formulation) and cooling rate [97]. It also has to be noted that up-scaling from droplet size samples to volumes of 1–5 Liters has an impact on the general freezing and thawing (e.g. location of highest cryoconcentration, formation of ice fronts) behavior but does not influence the ice crystal morphology (providing that the same cooling and heating rates are applied), initial melting and glass transition temperature. Nonetheless, our findings here show clearly that the ice crystal morphology and the glass transition temperatures can be tuned based on the choice of cryoprotectant. In fact, three categories can be distinguished, where either the lower T_g' or the higher T_g' can be suppressed. Depending on the type of protein and desired storage temperature either one of the three groups might be the best choice.

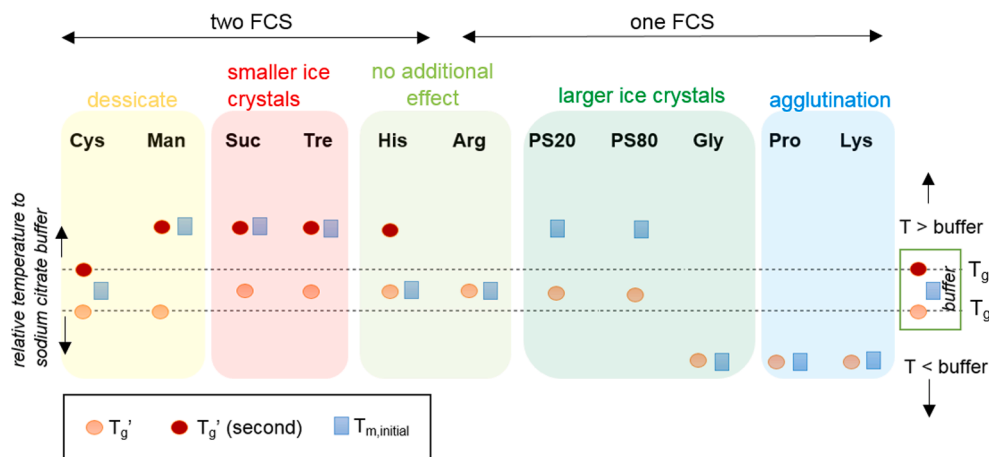


Fig. 9. Schematic depiction of all the effects cryoprotectants have when added to sodium citrate buffer. Note that the temperatures are not absolute, rather relative to the glass transition (T_g') and initial melting temperature ($T_{m,i}$) of the buffer solution!

As a follow-up study, we propose testing those three groups of cryoprotectants for their cryoprotective ability on therapeutic protein solutions by determining aggregate formation, using Size-Exclusion Chromatography after long-term storage. We believe that our approach can provide a valuable insight to multiple scientific research fields and industries and can support facilitation and optimization of cryopreservation methods.

5. Contributions

A.H. performed OCM and DSC measurements, A.H. and T.L. wrote the paper. T.L. and G.H. supervised the work.

Acknowledgements

We are grateful to the Austrian Science Fund FWF (Grant No. I1392) and Sandoz GmbH for financial support.

Appendix A. Supplementary material

Supplementary data to this article can be found online at <https://doi.org/10.1016/j.ejpb.2021.03.015>.

References

- C.D. Ball, C.R. Hardt, W.J. Duddles, The Influence of Sugars on the Formation of Sulfhydryl Groups in Heat Denaturation and Heat Coagulation of Egg Albumin, *J. Biol. Chem.* 151 (1943) 163–169, [https://doi.org/10.1016/S0021-9258\(18\)72124-8](https://doi.org/10.1016/S0021-9258(18)72124-8).
- S.L. Bradbury, W.B. Jakoby, Glycerol as an Enzyme-Stabilizing Agent: Effects on Aldehyde Dehydrogenase, *PNAS* 69 (1972) 2373–2376, <https://doi.org/10.1073/pnas.69.9.2373>.
- M.F. Utter, D.B. Keech, M.C. Scrutton, A possible role for acetyl CoA in the control of gluconeogenesis, *Adv. Enzyme Regul.* 2 (1964) 49–68, [https://doi.org/10.1016/S0065-2571\(64\)80005-4](https://doi.org/10.1016/S0065-2571(64)80005-4).
- R.P. Frigon, J.C. Lee, The stabilization of calf-brain microtubule protein by sucrose, *Arch. Biochem. Biophys.* 153 (1972) 587–589, [https://doi.org/10.1016/0003-9861\(72\)90376-1](https://doi.org/10.1016/0003-9861(72)90376-1).
- J.C. Lee, S.N. Timasheff, The stabilization of proteins by sucrose, *J. Biol. Chem.* 256 (1981) 7193–7201, [https://doi.org/10.1016/S0021-9258\(19\)68947-7](https://doi.org/10.1016/S0021-9258(19)68947-7).
- G.A. MacDonald, T.C. Lanier, in: M.C. Erickson, Y.C. Hung (Eds.), *Quality in Frozen Food*, Springer, Boston, MA, 1997, pp. 197–232. ISBN 9781461559757.
- T. Maity, A. Saxena, P.S. Raju, Use of hydrocolloids as cryoprotectant for frozen foods, *Crit. Rev. Food Sci. Nutr.* 58 (2018) 420–435, <https://doi.org/10.1080/10408398.2016.1182892>.
- P.J. Fellows, *Food Processing Technology*, fourth ed., Woodhead Publishing, Elsevier, 2017, pp. 885–928. ISBN 9780081019078.
- A.M. Kimulu, W.N. Mutuku, N.M. Mutua, Car Antifreeze and Coolant: Comparing Water and Ethylene Glycol as Nano Fluid Base Fluid, *Int. J. Adv. Sci. Res. Eng.* 4 (2018) 17–37, <https://doi.org/10.31695/IJASRE.2018.32748>.
- K.B.P.K. Reddy, S.P. Awasthi, A.N. Madhu, S.G. Prapulla, Role of Cryoprotectants on the Viability and Functional Properties of Probiotic Lactic Acid Bacteria during Freeze Drying, *Food Biotechnol.* 23 (2009) 243–265, <https://doi.org/10.1080/08905430903106811>.
- D.D. Oskouei, N. Bekmen, H. Ellidokuz, O. Yilmaz, Evaluation of different cryoprotective agents in maintenance of viability of *Helicobacter pylori* in stock culture media, *Braz. J. Microbiol.* 41 (2010) 1038–1046, <https://doi.org/10.1590/S1517-838220100004000023>.
- K. Hornberger, G. Yu, D. McKenna, A. Hubel, Cryopreservation of Hematopoietic Stem Cells: Emerging Assays, Cryoprotectant Agents, and Technology to Improve Outcomes, *Transfus. Med. Hemother.* 46 (2019) 188–196, <https://doi.org/10.1159/000496068>.
- J.L. Chaytor, J.M. Tokarew, L.K. Wu, M. Leclère, R.Y. Tam, C.J. Capicciotti, L. Guolla, E. von Moos, C.S. Findlay, D.S. Allan, R.N. Ben, Inhibiting ice recrystallization and optimization of cell viability after cryopreservation, *Glycobiology* 22 (2012) 123–133, <https://doi.org/10.1093/glycob/cwr115>.
- M. Schauerl, M. Podewitz, T.S. Ortner, F. Waibel, A. Thoery, T. Loerting, K. R. Liedl, Balance between hydration enthalpy and entropy is important for ice binding surfaces in Antifreeze Proteins, *Sci. Rep.* 7 (2017) 11901, <https://doi.org/10.1038/s41598-017-11982-8>.
- P.L. Davies, C.L. Hew, G.L. Fletcher, Fish antifreeze proteins: Physiology and evolutionary biology, *Can. J. Zool.* 66 (1988) 2611–2617, <https://doi.org/10.1139/z88-385>.
- J.G. Duman, Animal ice-binding (antifreeze) proteins and glycolipids: an overview with emphasis on physiological function, *J. Exp. Biol.* 218 (2015) 1846–1855, <https://doi.org/10.1242/jeb.116905>.
- A. Hauptmann, K. Podgoršek, D. Kuzman, S. Srdić, G. Hoelzl, T. Loerting, Impact of Buffer, Protein Concentration and Sucrose Addition on the Aggregation and Particle Formation during Freezing and Thawing, *Pharm. Res.* 35 (2018) 101, <https://doi.org/10.1007/s11095-018-2378-5>.
- P. Sundaramurthi, R. Suryanarayanan, The Effect of Crystallizing and Non-crystallizing Cosolutes on Succinate Buffer Crystallization and the Consequent pH Shift in Frozen Solutions, *Pharm. Res.* 28 (2011) 374–385, <https://doi.org/10.1007/s11095-010-0282-8>.
- M.J. Pikal, in: L. Rey, J.C. May (Eds.), *Freeze-Drying/Lyophilization of Pharmaceutical and Biological Products*, CRC Press, Boca Raton, ISBN 9780429215377, 2004, pp. 161–198.
- J.F. Carpenter, K.-I. Izutsu, T.W. Randolph, in: L. Rey, J.C. May (Eds.), *Freeze-Drying/Lyophilization of Pharmaceutical and Biological Products*, CRC Press, Boca Raton, 2004, pp. 167–197. ISBN 9780429215377.
- T. Arakawa, S.J. Prestrelski, W.C. Kenney, J.F. Carpenter, Factors affecting short-term and long-term stabilities of proteins, *Adv. Drug Deliv. Rev.* 46 (2001) 307–326, [https://doi.org/10.1016/S0169-409X\(00\)00144-7](https://doi.org/10.1016/S0169-409X(00)00144-7).
- F. Franks, *Biophysics and biochemistry at low temperatures*, Cambridge University Press, 1985. ISBN 9780521269322.
- L. Slade, H. Levine, D.S. Reid, Beyond water activity: Recent advances based on an alternative approach to the assessment of food quality and safety, *Crit. Rev. Food Sci. Nutr.* 30 (1991) 115–360, <https://doi.org/10.1080/10408399109527543>.
- K. Gekko, S.N. Timasheff, Mechanism of protein stabilization by glycerol: preferential hydration in glycerol-water mixtures, *Biochemistry* 20 (1981) 4667–4676, <https://doi.org/10.1021/bi00519a023>.
- T. Arakawa, S.N. Timasheff, The stabilization of proteins by osmolytes, *Biophys. J.* 47 (1985) 411–414, [https://doi.org/10.1016/S0006-3495\(85\)83932-1](https://doi.org/10.1016/S0006-3495(85)83932-1).
- G. Xie, S.N. Timasheff, Mechanism of the stabilization of ribonuclease A by sorbitol: Preferential hydration is greater for the denatured than for the native protein, *Protein Sci.* 6 (1997) 211–221, <https://doi.org/10.1002/pro.5560060123>.
- K. Izutsu, S. Yoshioka, T. Terao, Effect of Mannitol Crystallinity on the Stabilization of Enzymes during Freeze-Drying, *Chem. Pharm. Bull.* 42 (1994) 5–8, <https://doi.org/10.1248/cpb.42.5>.
- K. Izutsu, S. Kojima, Excipient crystallinity and its protein-structure-stabilizing effect during freeze-drying, *J. Pharm. Pharmacol.* 54 (2002) 1033–1039, <https://doi.org/10.1211/002235702320266172>.
- D.M. Piedmonte, C. Summers, A. McAuley, L. Karamujic, G. Ratnaswamy, Sorbitol crystallization can lead to protein aggregation in frozen protein formulations, *Pharm. Res.* 24 (2007) 136–146, <https://doi.org/10.1007/s11095-006-9131-1>.
- M.A. Mensink, H.W. Frijlink, K. van der Voort Maarschalk, W.L.J. Hinrichs, How sugars protect proteins in the solid state and during drying (review): Mechanisms of stabilization in relation to stress conditions, *Eur. J. Pharm. Biopharm.* 114 (2017) 288–295, <https://doi.org/10.1016/j.ejpb.2017.01.024>.
- J.F. Carpenter, M.J. Pikal, B.S. Chang, T.W. Randolph, Rational Design of Stable Lyophilized Protein Formulations: Some Practical Advice, *Pharm. Res.* 14 (1997) 969–975, <https://doi.org/10.1023/a:1012180707283>.
- P. Sundaramurthi, T.W. Patapoff, R. Suryanarayanan, Crystallization of trehalose in frozen solutions and its phase behavior during drying, *Pharm. Res.* 27 (2010) 2374–2383, <https://doi.org/10.1007/s11095-010-0243-2>.
- B.D. Connolly, L. Le, T.W. Patapoff, M.E.M. Cromwell, J.M.R. Moore, P. Lam, Protein Aggregation in Frozen Trehalose Formulations: Effects of Composition, Cooling Rate, and Storage Temperature, *J. Pharm. Sci.* 104 (2015) 4170–4184, <https://doi.org/10.1002/jps.24646>.
- G.B. Strambini, E. Gabellieri, Proteins in frozen solutions: Evidence of ice-induced partial unfolding, *Biophys. J.* 70 (1996) 971–976, [https://doi.org/10.1016/S0006-3495\(96\)79640-6](https://doi.org/10.1016/S0006-3495(96)79640-6).
- L. Zhang, X. Xue, J. Yan, L.-Y. Yan, X.-H. Jin, X.-H. Zhu, Z.-Z. He, J. Liu, R. Li, J. Qiao, L-proline: a highly effective cryoprotectant for mouse oocyte vitrification, *Sci. Rep.* 6 (2016) 26326, <https://doi.org/10.1038/srep26326>.
- V. Kostál, P. Šimek, H. Zahradníčková, J. Cimlová, T. Stětina, Conversion of the chill susceptible fruit fly larva (*Drosophila melanogaster*) to a freeze tolerant organism, *PNAS* 109 (2012) 3270–3274, <https://doi.org/10.1073/pnas.1119986109>.
- L.G. Sanchez-Partida, B.P. Setchell, W.M.C. Maxwell, Effect of compatible solutes and diluent composition on the post-thaw motility of ram sperm, *Reprod. Fertil. Dev.* 10 (1998) 347–358, <https://doi.org/10.1071/r98053>.
- J. Toxopeus, V. Kostál, B.J. Sinclair, Evidence for non-colligative function of small cryoprotectants in a freeze-tolerant insect, *Proc. R. Soc. B* 286 (2019), <https://doi.org/10.1098/rspb.2019.0050>.
- D. Freimark, C. Sehl, C. Weber, K. Hudel, P. Czermak, N. Hofmann, R. Spindler, B. Glasmacher, Systematic parameter optimization of a Me(2)SO- and serum-free cryopreservation protocol for human mesenchymal stem cells, *Cryobiology* 63 (2011) 67–75, <https://doi.org/10.1016/j.cryobiol.2011.05.002>.
- H. Sun, B. Glasmacher, N. Hofmann, Compatible solutes improve cryopreservation of human endothelial cells, *Cryo Lett.* 33 (2012) 485–493. PMID: 23250408.
- T.A. Pemberton, B.R. Still, E.M. Christensen, H. Singh, D. Srivastava, J.J. Tanner, Proline: Mother Nature's cryoprotectant applied to protein crystallography, *Acta Crystallogr. D Biol. Crystallogr.* 68 (2012) 1010–1018, <https://doi.org/10.1107/S0907444912019580>.
- A.S. Rudolph, J.H. Crowe, A calorimetric and infrared spectroscopic study of the stabilizing solute proline, *Biophys. J.* 50 (1986) 423–430, [https://doi.org/10.1016/S0006-3495\(86\)83478-6](https://doi.org/10.1016/S0006-3495(86)83478-6).
- R.J. Sundberg, R.B. Martin, Interactions of histidine and other imidazole derivatives with transition metal ions in chemical and biological systems, *Chem. Rev.* 74 (1974) 471–517, <https://doi.org/10.1021/cr60290a003>.
- T. Österberg, T. Wadsten, Physical state of L-histidine after freeze-drying and long-term storage, *Eur. J. Pharm. Sci.* 8 (1999) 301–308, [https://doi.org/10.1016/S0928-0987\(99\)00028-7](https://doi.org/10.1016/S0928-0987(99)00028-7).

- [45] J.P. Greenstein, M. Winitz. *Chemistry of the Amino Acids*, Wiley, New York, 1961, pp. 560–681. ISBN 9780471326373.
- [46] A. Al-Hussein, H. Gieseler, Investigation of histidine stabilizing effects on LDH during freeze-drying, *J. Pharm. Sci.* 102 (2013) 813–826, <https://doi.org/10.1002/jps.23427>.
- [47] T. Arakawa, D. Ejima, K. Tsumoto, N. Obeyama, Y. Tanaka, Y. Kita, S.N. Timasheff, Suppression of protein interactions by arginine: a proposed mechanism of the arginine effects, *Biophys. Chem.* 127 (2007) 1–8, <https://doi.org/10.1016/j.bpc.2006.12.007>.
- [48] V. Kostál, J. Korbellová, R. Poupardin, M. Moos, P. Šimek, Arginine and proline applied as food additives stimulate high freeze tolerance in larvae of *Drosophila melanogaster*, *J. Exp. Biol.* 219 (2016) 2358–2367, <https://doi.org/10.1242/jeb.142158>.
- [49] T. Arakawa, K. Tsumoto, The effects of arginine on refolding of aggregated proteins: not facilitate refolding, but suppress aggregation, *Biochem. Biophys. Res. Commun.* 304 (2003) 148–152, [https://doi.org/10.1016/s0006-291x\(03\)00578-3](https://doi.org/10.1016/s0006-291x(03)00578-3).
- [50] W.E.S. Carr, J.C. Netherton III, R.A. Gleeson, C.D. Derby, Stimulants of Feeding Behavior in Fish: Analyses of Tissues of Diverse Marine Organisms, *Biol. Bull.* 190 (1996) 149–160, <https://doi.org/10.2307/1542535>.
- [51] F. Emami, A. Vatanara, E.J. Park, D.H. Na, Drying Technologies for the Stability and Bioavailability of Biopharmaceuticals, *Pharmaceutics* 10 (2018) 131, <https://doi.org/10.3390/pharmaceutics10030131>.
- [52] A. Tariq, M. Ahmad, S. Iqbal, M.I. Riaz, M.Z. Tahir, A. Ghafoor, A. Riaz, Effect of carboxylated poly L-Lysine as a cryoprotectant on post-thaw quality and in vivo fertility of Nili Ravi buffalo (*Bubalus bubalis*) bull semen, *Theriogenology* 144 (2020) 8–15, <https://doi.org/10.1016/j.theriogenology.2019.12.012>.
- [53] Y. Tsuji, T. Iwasaki, H. Ogata, Y. Matsumoto, S. Koikeguchi, K. Matsumura, S. H. Hyon, M. Shiotani, The Beneficial Effect of Carboxylated Poly-L-Lysine on Cryosurvival of Vitriified Early Stage Embryos, *Cryo Letters* 38 (2017) 1–6. PMID: 28376134.
- [54] D.A. Vorontsov, G. Sazaki, S.-H. Hyon, K. Matsumura, Y. Furukawa, Antifreeze Effect of Carboxylated ϵ -Poly-L-lysine on the Growth Kinetics of Ice Crystals, *J. Phys. Chem. B* 118 (2014) 10240–10249, <https://doi.org/10.1021/jp507697q>.
- [55] A. Henao, G.N. Ruiz, N. Steinke, S. Cervený, R. Macovez, E. Guàrdia, S. Busch, S. E. McLain, C.D. Lorenz, L.C. Pardo, On the microscopic origin of the cryoprotective effect in lysine solutions, *PCCP* 22 (2020) 6919–6927, <https://doi.org/10.1039/C9CP06192D>.
- [56] A. Mukunoki, T. Takeo, N. Nakagata, N-acetyl cysteine restores the fertility of vitriified-warmed mouse oocytes derived through ultrasuperovulation, *PLoS ONE* 14 (2019), e0224087, <https://doi.org/10.1371/journal.pone.0224087>.
- [57] S. Iqbal, A. Riaz, S.M.H. Andrabi, Q. Shahzad, A.Z. Durrani, N. Ahmad, L-Cysteine improves antioxidant enzyme activity, post-thaw quality and fertility of Nili-Ravi buffalo (*Bubalus bubalis*) bull spermatozoa, *Andrologia* 48 (2016) 855–861, <https://doi.org/10.1111/and.12520>.
- [58] B. Khalili, M. Jafaroghli, A. Farshad, M. Paresh-Khiavi, The Effects of Different Concentrations of Glycine and Cysteine on the Freezability of Moghani Ram Spermatozoa, *Asian-Australas. J. Anim. Sci.* 23 (2010) 318–325, <https://doi.org/10.5713/ajas.2010.90387>.
- [59] W. Jung, R.L. Campbell, Y. Gwak, J.I. Kim, P.L. Davies, E. Jin, New Cysteine-Rich Ice-Binding Protein Secreted from Antarctic Microalgae, *Chloromonas* sp., *PLoS One* 11 (2016), e0154056, <https://doi.org/10.1371/journal.pone.0154056>.
- [60] L. Kreilgaard, L.S. Jones, T.W. Randolph, S. Frokjaer, J.M. Flink, M.C. Manning, J. F. Carpenter, Effect of Tween 20 on freeze-thawing- and agitation-induced aggregation of recombinant human factor XIII, *J. Pharm. Sci.* 87 (1998) 1593–1603, <https://doi.org/10.1021/js980126i>.
- [61] B.A. Kerwin, Polysorbates 20 and 80 used in the formulation of protein biotherapeutics: Structure and degradation pathways, *J. Pharm. Sci.* 97 (2008) 2924–2935, <https://doi.org/10.1002/jps.21190>.
- [62] M. Dombrow, E. Azaz, A. Pillersdorf, Autoxidation of polysorbates, *J. Pharm. Sci.* 67 (1978) 1676–1681, <https://doi.org/10.1002/jps.2600671211>.
- [63] H.D. Goff, Colloidal aspects of ice cream—A review, *Int. Dairy J.* 7 (1997) 363–373, [https://doi.org/10.1016/S0958-6946\(97\)00040-X](https://doi.org/10.1016/S0958-6946(97)00040-X).
- [64] A. Hauptmann, K.F. Handle, P. Baloh, H. Grothe, T. Loerting, Does the emulsification procedure influence freezing and thawing of aqueous droplets? *J. Chem. Phys.* 145 (2016), 211923 <https://doi.org/10.1063/1.4965434>.
- [65] M.B. Burg, J.D. Ferraris, Intracellular organic osmolytes: function and regulation, *J. Biol. Chem.* 283 (2008) 7309–7313, <https://doi.org/10.1074/jbc.R700042200>.
- [66] A.K. Parida, A.B. Das, Salt tolerance and salinity effects on plants: a review, *Ecotoxicol. Environ. Saf.* 60 (2005) 324–349, <https://doi.org/10.1016/j.ecoenv.2004.06.010>.
- [67] J.H. Crowe, L.M. Crowe, Factors affecting the stability of dry liposomes, *Biochim. Biophys. Acta, Biomembr.* 939 (1988) 327–334, [https://doi.org/10.1016/0005-2736\(88\)90077-6](https://doi.org/10.1016/0005-2736(88)90077-6).
- [68] J.B. Benoit, G. Lopez-Martinez, M.A. Elnitsky, R.E. Lee Jr, D.L. Denlinger, Dehydration-induced cross tolerance of Belgica antarctica larvae to cold and heat is facilitated by trehalose accumulation, *Comp. Biochem. Physiol. A Mol. Integr. Physiol.* 152 (2009) 518–523, <https://doi.org/10.1016/j.cbpa.2008.12.009>.
- [69] J.H. Crowe, L.M. Crowe, D. Chapman, Preservation of Membranes in Anhydrobiotic Organisms: The Role of Trehalose, *Science* 223 (1984) 701–703, <https://doi.org/10.1126/science.223.4637.701>.
- [70] D.S. Neufeld, L.P. Leader, Freezing survival by isolated Malpighian tubules of the New Zealand alpine weta *Hemideina maori*, *J. Exp. Biol.* 201 (1998) 227–236. PMID: 9405309.
- [71] R.E. Johnson, C.F. Kirchoff, H.T. Gaud, Mannitol-sucrose mixtures - Versatile formulations for protein lyophilization, *J. Pharm. Sci.* 91 (2002) 914–922, <https://doi.org/10.1002/jps.10094>.
- [72] R.K. Cavatur, N.M. Vemuri, A. Pyne, Z. Chrzan, D. Toledo-Velasquez, R. Suryanarayanan, Crystallization behavior of mannitol in frozen aqueous solutions, *Pharm. Res.* 19 (2002) 894–900, <https://doi.org/10.1023/a:1016177404647>.
- [73] R.E. Lee Jr. *Low Temperature Biology of Insects*, Cambridge University Press, Cambridge, 2010, pp. 3–34. ISBN 9780521886352.
- [74] K.E. Marshall, B.J. Sinclair, The sub-lethal effects of repeated freezing in the woolly bear caterpillar *Pyrrharctia isabella*, *J. Exp. Biol.* 214 (2011) 1205–1212, <https://doi.org/10.1242/jeb.054569>.
- [75] P.H. Yancey, Organic osmolytes as compatible, metabolic and counteracting cytoprotectants in high osmolarity and other stresses, *J. Exp. Biol.* 208 (2005) 2819–2830, <https://doi.org/10.1242/jeb.01730>.
- [76] L.B. Lane, Freezing Points of Glycerol and Its Aqueous Solutions, *Ind. Eng. Chem.* 17 (1925) 924, <https://doi.org/10.1021/ie50189a017>.
- [77] A. Bogdan, M.J. Molina, H. Tenhu, E. Bertel, N. Bogdan, T. Loerting, Visualization of Freezing Process in situ upon Cooling and Warming of Aqueous Solutions, *Sci. Rep.* 4 (2014) 7414, <https://doi.org/10.1038/srep07414>.
- [78] A. Hauptmann, G. Hoelzl, T. Loerting, Distribution of Protein Content and Number of Aggregates in Monoclonal Antibody Formulation After Large-Scale Freezing, *Distribution of Protein Content and Number of Aggregates in Monoclonal Antibody Formulation After Large-Scale Freezing* 20 (2019) 72, <https://doi.org/10.1208/s12249-018-1281-z>.
- [79] H.H. Teng, How Ions and Molecules Organize to Form Crystals, *Elements* 9 (2013) 189–194, <https://doi.org/10.2113/gselements.9.3.189>.
- [80] C. Telang, L. Yu, R. Suryanarayanan, Effective Inhibition of Mannitol Crystallization in Frozen Solutions by Sodium Chloride, *Pharm. Res.* 20 (2003) 660–667, <https://doi.org/10.1023/A:1023263203188>.
- [81] P. Kolhe, E. Amend, S.K. Singh, Impact of freezing on pH of buffered solutions and consequences for monoclonal antibody aggregation, *Biotechnol. Prog.* 26 (2010) 727–733, <https://doi.org/10.1002/btpr.377>.
- [82] W. Hemminger, G. Höhne, *Grundlagen der Kalorimetrie*, WILEY-VCH Verlag GmbH, Weinheim, 1980. ISBN 978-3527258277.
- [83] P.H. Rasmussen, B. Jørgensen, J. Nielsen, Aqueous solutions of proline and NaCl studied by differential scanning calorimetry at subzero temperatures, *Thermochim. Acta* 303 (1997) 23–30, [https://doi.org/10.1016/S0040-6031\(97\)00241-4](https://doi.org/10.1016/S0040-6031(97)00241-4).
- [84] C.A. Angell, Liquid Fragility and the Glass Transition in Water and Aqueous Solutions, *Chem. Rev.* 102 (2002) 2627–2650, <https://doi.org/10.1021/cr000689q>.
- [85] A. Bogdan, M.J. Molina, H. Tenhu, T. Loerting, Multiple Glass Transitions and Freezing Events of Aqueous Citric Acid, *J. Phys. Chem. A* 119 (2015) 4515–4523, <https://doi.org/10.1021/jp510331h>.
- [86] B.S. Chang, C.S. Randall, Use of subambient thermal analysis to optimize protein lyophilization, *Cryobiology* 29 (1992) 632–656, [https://doi.org/10.1016/0011-2240\(92\)90067-C](https://doi.org/10.1016/0011-2240(92)90067-C).
- [87] L. Slade, H. Levine, Non-equilibrium behavior of small carbohydrate-water systems, *Pure Appl. Chem.* 60 (1988) 1841–1864, <https://doi.org/10.1351/pac198860121841>.
- [88] B. Zobrist, V. Soonsin, B.P. Luo, U.K. Krieger, C. Marcolli, T. Peter, T. Koop, Ultra-slow water diffusion in aqueous sucrose glasses, *PCCP* 13 (2011) 3514–3526, <https://doi.org/10.1039/c0cp01273d>.
- [89] M. Xu, G. Chen, C. Zhang, S. Zhang, Study on the Unfrozen Water Quantity of Maximally Freeze-Concentrated Solutions for Multicomponent Lyoprotectants, *J. Pharm. Sci.* 106 (2017) 83–91, <https://doi.org/10.1016/j.xphs.2016.05.007>.
- [90] A.P. Whelan, A. Regand, C. Vega, J.P. Kerry, H.D. Goff, Effect of trehalose on the glass transition and ice crystal growth in ice cream, *Int. J. Food Sci. Tech.* 43 (2008) 510–516, <https://doi.org/10.1111/j.1365-2621.2006.01484.x>.
- [91] K.D. Roe, T.P. Labuza, Glass Transition and Crystallization of Amorphous Trehalose-sucrose Mixtures, *Int. J. Food Prop.* 8 (2005) 559–574, <https://doi.org/10.1080/10942910500269824>.
- [92] C.A. Knight, E. Driggers, A.L. DeVries, Adsorption to ice of fish antifreeze glycopeptides 7 and 8, *Biophys. J.* 64 (1993) 252–259, [https://doi.org/10.1016/s0006-3495\(93\)81361-4](https://doi.org/10.1016/s0006-3495(93)81361-4).
- [93] A.I. Kim, M.J. Akers, S.L. Nail, The physical state of mannitol after freeze-drying: Effects of mannitol concentration, freezing rate, and a noncrystallizing cosolute, *J. Pharm. Sci.* 87 (1998) 931–935, <https://doi.org/10.1021/js980001d>.
- [94] A. Martini, S. Kume, M. Crivellente, R. Artico, Use of subambient differential scanning calorimetry to monitor the frozen-state behavior of blends of excipients for freeze-drying, *PDA J. Pharm. Sci. Technol.* 51 (1997) 62–67. PMID: 9146035.
- [95] A. Hillgren, J. Lindgren, M. Alden, Protection mechanism of Tween 80 during freeze-thawing of a model protein, LDH, *Int. J. Pharm.* 237 (2002) 57–69, [https://doi.org/10.1016/s0378-5173\(02\)00021-2](https://doi.org/10.1016/s0378-5173(02)00021-2).
- [96] B. Schobert, H. Tschesche, Unusual solution properties of proline and its interaction with proteins, *Biochim. Biophys. Acta, Gen. Subj.* 541 (1978) 270–277, [https://doi.org/10.1016/0304-4165\(78\)90400-2](https://doi.org/10.1016/0304-4165(78)90400-2).
- [97] M.A. Miller, M.A. Rodrigues, M.A. Glass, S.K. Singh, K.P. Johnston, J.A. Maynard, Frozen-state storage stability of a monoclonal antibody: Aggregation is impacted by freezing rate and solute distribution, *J. Pharm. Sci.* 102 (2013) 1194–1208, <https://doi.org/10.1002/jps.23473>.